Sustainable Removal of Total Dissolved Solids from Paint Wastewater Using Avocado Pear and Moringa Oleifera Seed Bio–Coagulants Through an Adsorption–Assisted Coagulation–Flocculation Process

Cyprian O. Azinta[1*], Onyekachi S. Nnamani[1], Ogochukwu C. Nevo[1](0009-0004-9174-9873)

[1]*Department of Chemical Engineering, Enugu State University of Science and Technology, Enugu, Nigeria*

*Corresponding author: azinta.acom@gmail.com *ORCID: 0009-0009-7357-3153

Abstract

In this study, avocado pear seed (PS) and moringa oleifera seed (MOS) were processed and characterized by proximate analysis, Fourier transform infrared (FTIR) spectroscopy, and point of zero charge (pHpzc) determination before they were applied as bio-coagulants for the treatment of paint wastewater (PWW) with high total dissolved solids (TDS). Coagulation–flocculation was employed as the primary treatment mechanism, with adsorption investigated as a complementary removal process. The characterization confirmed the presence of functional groups, protein and carbohydrate associated with coagulation–flocculation, and the relatively high pHpzc values implied positively charged bio-coagulant surfaces at the optimum treatment pH, which enabled charge neutralization and electrostatic attraction of dissolved species. The effects of pH, coagulant dosage and contact time on TDS removal were studied using coagulation–flocculation tests. The initial TDS concentration of the raw PWW decreased from 2524.43 mg L^{-1} to 165.54 mg L^{-1} (93% removal) and to 100.13 mg L^{-1} (96% removal) after treatment with PS and MOS respectively. The treatment data were subjected to adsorption, kinetic, diffusion, and equilibrium isotherm analyses. The analyses revealed that both bio-coagulants followed the pseudo-second-order kinetic ($R^2 > 0.98$) and the Langmuir isotherm ($R^2 > 0.99$) models, showing that adsorption was mainly through surface interactions on available active sites. Although MOS achieved a higher overall TDS removal, PS exhibited slightly more favourable adsorption behaviour. These results show the potential of avocado pear seed and moringa oleifera seed bio-coagulants as promising, biodegradable and environmentally sustainable alternatives to the conventional chemical coagulants for industrial wastewaters treatment.

Keywords: total dissolved solids removal; paint wastewater; bio-coagulants; adsorption-assisted coagulation–flocculation; adsorption isotherms; adsorption kinetics; intra-particle diffusion

1. Introduction

With the rapid rise of industry, the quantity of wastewater generated by production processes has increased dramatically. Effluents from such industries especially in paint industries are usually rich in solids such as total dissolved solids (TDS) and contain complex mixture of stabilizers, pigment, toxic ions, surfactants and other stubborn compounds that pose serious risk to the public health and environment [1], [2]. High percentage of TDS levels in waste water results to huge volumes of salt, limit light penetration in receiving water bodies and can affect aquatic life. It also

causes a risk of contaminating ground water and agricultural soils [3]. Due to this, discharge rules for industrial effluents in most of the urban cities have become stringent [3]. Treatment of paint wastewater (PWW) has generally been based on chemical coagulation-flocculation process using standard Jar test methods to establish appropriate coagulant dosages and mixing conditions as per the findings of [4], [5]. The most widely used coagulants are inorganic ones because they are efficient at destabilizing colloidal and suspended particles. The most common are aluminum and iron-based salts [5]. These chemicals are efficient but produce huge amounts of sludge and may also cause residual metal ions in the treated wastewater, raising concerns over secondary contamination and increasing the expense and complexity of sludge management as reported in [1], [2], [3], [5]. These problems have been a driving force behind increased research interest in more sustainable and biodegradable treatment alternatives.

Plant-based coagulants, also known as bio-coagulants, are gaining attention as environmentally friendly alternatives to treat wastewater due to their biodegradability, availability, low cost, and smaller environmental footprints than traditional chemical coagulants [1], [2], [3], [4], [5]. The recent study by Miyah et al. [6], Jabar et al. [7] and Zhang et al. [8] on green remediation materials stressed the increasing importance of sustainable adsorbents and bio-based treatment technologies in wastewater purification. The active components of the plant seed derived materials, avocado pear seed (PS) and moringa oleifera seed (MOS) promote both coagulation–flocculation and adsorption processes [9]. For example, studies reported by [9], [10] indicate that PS consists primarily of polysaccharides and lignocellulosic matter that contribute to particle bridging and aggregation, whereas MOS includes cationic proteins and charged functional groups that facilitate electrostatic attraction and binding of dissolved substances. Moreover, these plant-based materials possess substantial adsorption capacity for dissolved particles besides their coagulating ability which makes them good candidates to reduce TDS in complex industrial effluents [10]. As stated by Obiora-Okafo et al. [11], functional groups are important because the performance of adsorption-based treatment systems depends on surface functional groups, electrostatic interactions, adsorption kinetics, and mass transfer processes that influence the contaminant removal efficiency and uptake.

Many studies [12], [13], [14] have proved the effectiveness of bio-coagulants for the reduction of turbidity, colour and chemical oxygen demand in wastewater, but limited studies are available on TDS removal from paint wastewater by a synergistic adsorption-assisted coagulation-flocculation process. Moreover, most of the published research are focused on the efficiency of the treatment and there is limited detailed mechanistic explanation based on adsorption isotherms, kinetic modelling, diffusion analysis and surface-charge characterization [13], [14]. Understanding the adsorption kinetics is important, as it helps in identification of rate controlling steps, better prediction of the system performance, comparison of different coagulants used and optimization of process conditions for possible scale-up [15], [16], [17].

[16], [18] described pseudo first and second order kinetic models are most commonly utilized for the description and deduction of adsorption behavior and governing mechanisms. Specifically, the pseudo-first-order model is related to physisorption, which includes weaker attraction forces such van der Waals forces, hydrogen bonding, or electrostatic attraction, without significant electron

exchange or bond formation [18]. The pseudo-second order model is related to chemisorption in which there are stronger interactions with sharing or exchange of electrons between functional groups on the surface of the adsorbent and the species of the adsorbate [19]. [20] showed that the Elovich model is useful for systems with heterogeneous surfaces and varying activation energies. These models provide the possibility to quantitatively estimate characteristics such as adsorption capacity and rate constants which are needed for the comparison of processes and the design of full-scale systems [16], [18], [19], [20].

The mass transfer processes are important to the effectiveness of treatment process besides the surface reaction kinetics. This is where the Weber–Morris intra-particle diffusion model is used. The model is mainly applied to determine if the rate of adsorption is controlled by the diffusion within the pores of an adsorbent [21]. In [22] it is pointed out that adsorption rarely occurs in a single step but follows a sequence which starts with external mass transfer over the boundary layer (film diffusion), followed by intra-particle diffusion and lastly equilibrium adsorption. The non-zero intercepts of the linear plots of Weber-Morris model are attributed to the combined effect of boundary-layer resistance and intra-particle diffusion. Then, the slope of the figure reveals the intra-particle diffusion rate constant and the intercept gives an idea about the magnitude of film diffusion effects [21], [22]. Understanding these transport phases is critical for the identification of rate restrictions and to improve the treatment efficiency of the process [2].

Isotherm analysis apart from adsorption kinetics gives highly crucial information on adsorption capacity, surface properties and type of adsorbent-adsorbate interactions [15], [23]. Commonly used models are the Langmuir isotherm which assumes monolayer adsorption on a homogeneous surface with finite active sites [15], and the Freundlich isotherm which explains adsorption on heterogeneous surfaces with variable adsorption energies [23]. The Temkin isotherm addresses the adsorbent-adsorbate interactions and assumes that the heat of adsorption reduces linearly with the increase of the surface covering [24]. Therefore, isotherm modelling can contribute to understand the adsorption mechanisms and the feasibility of adsorbent materials for applications in wastewater treatment.

Unlike previous studies that primarily focus on one bio-coagulant or adsorbent for pollutant removal from different industrial effluents [9], [10], [12], [13], [14], the present study is focused on the utilization and comparative evaluation of two readily available and low-cost plant-based bio-coagulants, PS and MOS for the treatment of paint wastewater with high concentration of TDS using adsorption assisted coagulation-flocculation technique. The paper also discusses the mechanisms involved in TDS removal under different operating settings such as pH, coagulant dosage and contact time as well as the treatment performance. It should be noted that the exerimental system investigated in the present study is the same as that reported in our previous publication, which focused on the optimization and predictive modelling of TDS removal using response surface methodology (RSM) and artificial neural network (ANN) [25]. In contrast, the objectives of this study are fundamentally different, which include to: (i) assess the effectiveness of PS and MOS as sustainable bio-coagulants for TDS removal from paint wastewater; (ii) optimize the coagulation–flocculation process by investigating the effect of pH, bio-coagulant dosage and contact time on TDS removal; (iii) characterize the bio-coagulants and determine their

surface properties through proximate analysis, Fourier transform infrared (FTIR) spectroscopy and point of zero charge (pHpzc); (iv) analyze the contribution of adsorption through adsorption capacity, isotherm, kinetic and Weber–Morris intra-particle diffusion analyses; and (v) compare the performance of PS and MOS and suggest a mechanistic pathway for TDS removal from paint wastewater. The findings of this study could support the development of sustainable and low-cost treatment systems for industrial wastewater management, particularly in regions where conventional chemical coagulants are costly or less accessible.

2. Materials and Methods

2.1 Equipment, Reagents, and Bio-Coagulant Preparation

The experiments were conducted utilizing laboratory equipment such as mortar and pestle, graduated cylinders, beakers, electronic balance, magnetic stirrer, pH meter, oven and Whatman No. 1 filter paper. The mixing and settling periods during the jar tests procedures were recorded using a stopwatch. The primary materials used were avocado pear seeds (PS), moringa oleifera seeds (MOS) and paint wastewater (PWW). pH correction was also carried out using distilled water, sodium hydroxide, hydrochloric acid, ethylenediaminetetraacetic acid (EDTA) and appropriate buffer solutions. Impurities were washed away from the seed materials, then dried in an oven at 60 °C for 24 hours. They were dried, milled to powder and sieved to get a homogeneous particle size by the methods described in [26]. The resultant powders were employed as bio-coagulant and stored in sealed containers at room temperature till when needed.

2.2 Sampling of Paint Wastewater

Paint wastewater (PWW) was obtained from an offline storage tank at Legacy Paints Limited, located in the Emene Industrial Layout, Enugu, Nigeria. After collection, the samples were kept at 4 °C and analyzed within 24 hours to preserve their stability. The initial TDS concentration was determined before any treatment was applied.

2.3 Treatment Mechanism and Experimental Approach

In this work, the coagulation–flocculation process was examined as the main mechanism. We also evaluated adsorption as a supplementary mechanism contributing to TDS removal due to the fact that PS and MOS bio-coagulants include surface functional groups which are capable of interacting with dissolved species. The bio-coagulants were characterized by FTIR and pHpzc investigations and their adsorption behavior was evaluated by contact-time studies, kinetics, and equilibrium isotherm modeling to estimate the impact of these bio-coagulants.

2.3.1 Coagulation–flocculation experiments

The influence of operating parameters on TDS removal from paint wastewater was studied by jar test experiments in 500 mL beakers under controlled laboratory settings using the approach described in [26]. The effect of three important operational factors (pH, bio-coagulant dosage and

contact time) was examined. The effluent was adjusted to pH 2, 4, 6, 8 and 10 prior to treatment. Bio-coagulant doses were 1, 2, 3, 4 and 5 g per 500mL of waste water with initial TDS content of 200 mg/L. Contact time was assessed at 10, 20, 30, 40 and 50 min. The dose of bio-coagulant required for each experiment was added to 500 mL of wastewater in a beaker at room temperature. The coagulation-flocculation process comprised of rapid mixing (150 rpm, 2 min), moderate mixing (40 rpm, 20 min) and settling under quiescent circumstances. Aliquots were taken at 10 min intervals up to 50 min after treatment to investigate the effect of contact time on TDS removal kinetics. The TDS concentration of each sample was determined and the removal efficiency was computed using the Equation (1) [25]:

$$TDS\ removal\ (\%) = \frac{C_0 - C_t}{C_0} \times 100 \qquad (1)$$

where C_0 is the initial TDS concentration (mg/L) and C_t is the final TDS concentration (mg/L) after coagulation–flocculation treatment. The optimum operational settings derived from the experimental investigation were further validated by independent verification studies.

2.4 Optimum Operating Conditions and Validation

To validate the optimum operating parameters obtained from the experimental study, validation experiments were performed at the predicted optimum pH, dosage, and contact time. The experimental TDS removal efficiencies were compared with the corresponding predicted values, and the percentage deviation was calculated to evaluate the accuracy and reproducibility of the treatment procedure.

2.5 Bio-Coagulant and Wastewater Characterization

The physicochemical properties of the bio-coagulants and paint wastewater were characterized to provide information on their composition, surface chemistry, charge behavior, and treatment potential. Proximate composition analysis, FTIR, pHpzc determination, and wastewater characterization were carried out using standard analytical procedures.

2.5.1 Proximate composition analysis

Selected proximate composition of PS and MOS including protein, carbohydrate, moisture, ash contents, surface area and yield were determined using procedure of [27]. The investigation was undertaken to evaluate the compositional properties of the bio-coagulants and their potential influence on coagulation–flocculation and adsorption processes.

2.5.2 Fourier transform infrared (FTIR) analysis

Functional groups responsible for adsorption, charge neutralization, and pollutant binding during wastewater treatment were identified using FTIR spectroscopy. FTIR analysis was performed in the selected wavenumber range and the obtained spectra confirmed the presence of functional groups.

2.5.3 Point of zero charge (pHpzc) determination

The pH point of zero charge (pHpzc) of PS and MOS was found using the pH drift method. Solutions with different initial pH values were prepared and contacted with the bio-coagulants until equilibrium was attained. The pHpzc was obtained from the intersection of the ΔpH versus initial pH (pHi) plot at ΔpH = 0. The surface charge properties of bio-coagulants and their interaction with dissolved species at different pH settings were studied by the pHpzc.

2.5.4 Physicochemical Characterization of Paint Wastewater

The performance of the bio-coagulants was evaluated by characterising the paint wastewater before and after treatment. The parameters total solids (TS), total suspended solids (TSS), total dissolved solids (TDS), chemical oxygen demand (COD), biological oxygen demand (BOD5), pH and electrical conductivity were measured according to conventional procedures [10], [12], [13], [28].

2.6 Adsorption Capacity, Kinetic and Diffusion Models

2.6.1 Adsorption capacity

Adsorption capacities were calculated from the experimental data to explore the role of adsorption in TDS removal during coagulation-flocculation treatment, and fitted to kinetic and diffusion models. The adsorption capacity at time t (q_t) and the equilibrium adsorption capacity (q_e) of PS and MOS for TDS removal were calculated using Equations (2) and (3), respectively [22, 29]:

$$q_t = \frac{(C_0 - C_t)V}{m} \quad (2)$$

$$q_e = \frac{(C_0 - C_e)V}{m} \quad (3)$$

where C_e is the equilibrium TDS concentration (mg/L), V is the solution volume (L) and m is the mass of bio-coagulant (g).

2.6.2 Kinetic models

The experimental TDS removal data were fitted to kinetic models to understand the adsorption mechanism by using pseudo-first-order (PFO), pseudo-second-order (PSO), Elovich and Weber–Morris intra-particle diffusion models. Rate constants and model parameters for PFO, PSO and Elovich were obtained from linearized graphical plots according to Equations (4), (5) and (6), respectively [21, 29]:

$$ln\ ln\left(q_t - q_e\right) = ln\ ln\ q_e - K_1 t \quad (4)$$

$$\frac{t}{q_t} = \frac{1}{K_2 {q_e}^2} + \frac{t}{q_e} \quad (5)$$

$$q_t = \frac{1}{\beta} ln\ ln\ (1 + \alpha\beta t) \quad (6)$$

where t is the contact time (min), K_1 is the pseudo-first-order rate constant (min^{-1}), K_2 is the pseudo-second-order rate constant (g/mg·min), α is the initial adsorption rate (mg/g·min) and β is the desorption constant related to surface coverage (g/mg).

2.6.3 Diffusion model

The intra-particle diffusion rate constant, K_{id} (mg/g·$min^{0.5}$), was from the Weber–Morris intra-particle diffusion model generally given by the equation of (7) by plotting q_t vs $t^{\frac{1}{2}}$ [21, 29]. The slope of the plot gives K_{id}.

$$q_t\ = K_{id} t^{\frac{1}{2}} +\ C \quad (7)$$

where $t^{\frac{1}{2}}$ is the square root of time (min) and C is the intercept (mg/g) representing the thickness of the boundary layer.

2.7 Adsorption Isotherm Models

To further evaluate the nature of adsorbate-adsorbent interactions, the equilibrium data collected from coagulation-flocculation tests carried out at varied TDS concentrations were fitted to the adsorption isotherm models. The data were fitted to Langmuir, Freundlich and Temkin models to characterize the equilibrium connection between TDS adsorption capacity and residual concentration in solution, and also to analyze the adsorption mechanism and surface features of PS and MOS. The model parameters for Langmuir, Freundlich and Temkin were calculated from the linear plots of the transformed data according to Equations (8), (9) and (10) accordingly [23]:

$$\frac{C_e}{q_e} = \frac{1}{q_{max} K_L} + \frac{C_e}{q_{max}} \quad (8)$$

where C_e is the equilibrium concentration (mg/L), q_{max} is the maximum monolayer adsorption capacity (mg/g), and K_L is the Langmuir constant related to adsorption affinity (L/mg).

$$ln\ ln\ q_e\ = ln\ ln\ K_F\ + \frac{ln\ ln\ C_e}{n} \quad (9)$$

where K_F is the Freundlich adsorption capacity constant and $\frac{1}{n}$ represents adsorption intensity or surface heterogeneity.

$$q_e = B\ ln\ ln\ C_e\ + B\ ln\ ln\ A \quad (10)$$

where A is the Temkin equilibrium binding constant (L/g), and B is related to the heat of adsorption and adsorbate–adsorbent interactions.

3. Results and Discussion

3.1 Characterization of Bio-Coagulants and Paint Wastewater

The bio-coagulants were characterized for proximate composition as shown in Table 1. Significant difference was seen in protein and carbohydrate content. MOS had more protein (37.16%) than PS (18.96%), but PS contained more carbohydrate (53.08%) than MOS (44.63%). These results suggest that the presence of the MOS coagulant increased the electrostatic interactions and binding of the dissolved species present in the wastewater sample while the PS coagulant increased the adsorption processes [10], [30]. This behavior can be explained by their protein and carbohydrate composition. This conclusion agrees with what has been reported in the literature on bio-coagulants.

Table 1
Result of Proximate Composition of PS and MOS

Bio-coagulant	Protein content %	Carbohydrate content %	Moisture content %	Ash content %	Yield %
PS	18.96	53.08	9.75	2.23	25.63
MOS	37.16	44.63	9.04	2.43	30.52

From the FTIR spectra in Table 2, we can see that there were important functional groups such as hydroxyl (C-O stretch), carboxyl (C=O stretch), and amine (N-H bend and N-H stretch) groups engaged in the adsorption process. These functional groups are important for TDS removal, since they can interact with dissolved ions and organic matters commonly found in PWW [30].

Table 2
Result of FTIR of PS and MOS bio-coagulants for functional group identification

	PS			**MOS**	
Peak	**Functional group**	**Class of Compound**	**Peak**	**Functional group**	**Class of compound**
3283.8	≡≡C-H stretch	Alkynes	3693.8	N-H stretch	Amines
2918.5	C-H stretch	Alkanes and Alkyls	3287.5	≡≡C-H stretch	Alkynes
2851.4	C-H stretch	Alkanes and Alkyls	2918.5	C-H stretch	Alkanes and alkyls
2105.9	C≡≡C stretch	Alkynes	2851.4	C-H stretch	Alkanes and alkyls
1997.9	-	-	2117.1	C≡≡C Stretch	Alkynes
1953.1	-	-	1990.4	-	-
1733.2	C=O stretch	Aldehydes	1729.5	C=O stretch	Esters

1617.7	N-H bend	Amines	1610.2	N-H bend	Amines
1420.1	-	-	1438.8	-	-
1375.4	CH_3C-H bend	Alkanes and Alkyls	1367.9	-	-
1237.5	C-O stretch	Alcohol	1315.8	C-F stretch	Alkyl halides
1319.5	C-F stretch	Alkyl halides	1200.2	=C-O-C sym. & asym. Stretch	Ethers
1151.7	C-O stretch	Alcohol	1155.5	C-O stretch	Alcohol
779.0	C-H bend	Aromatic compound	779.0	C-H bend	Aromatic compound
1010.1	C-F stretch		663.5	≡≡C-H bend	Alkynes
-	-		1028.7	C-O stretch	Alcohol

The first assessment of the paint wastewater sample as shown in Table 3 showed a significantly polluted effluent with a high TDS value of 2524.43 mg/L. Other associated characteristics such as pH, COD, BOD5, Turbidity, pH and electrical conductivity additionally indicated the complexity of the effluent. The TDS concentrations were reduced to 165.54 mg/L and 100.13 mg/L by the treatment of PS and MOS, respectively, which is around 93% and 96% elimination. This result shows the efficiency of both bio-coagulants for treating paint effluent.

Table 3
Result of characterization of paint wastewater pre- and post-treatment

Parameter	TS mg/L	TSS mg/L	TDS mg/L	COD mg/L	BOD_5 mg/L	Turbidity NTU	pH	Conductivity µS/cm
Pre-treatment	2599.67	75.24	2524.43	2374.58	1586.11	48.17	6.16	509
Post-treatment, PS	171.87	6.33	165.54	215.82	172.67	3.383	6.33	96.05
Post-treatment, MOS	106.46	6.33	100.13	411.95	398.22	3.41	6.42	103.65

3.2 Effects of Process Parameters

3.2.1 Effects of pH on TDS removal

As shown in Figure 1, both PS and MOS were found to exhibit the highest TDS removal at pH 4 and the removal effectiveness declined gradually with the increase of pH. It can be noted that MOS performed somewhat better than PS in the examined pH range. To further understand the effect of pH on the surface functional groups of PS and MOS, the pHpzc measurement is needed. This explains the better elimination of pollutants under acidic conditions.

Figure 1:
Plot of TDS removal efficiency against pH for PS and MOS bio-coagulants

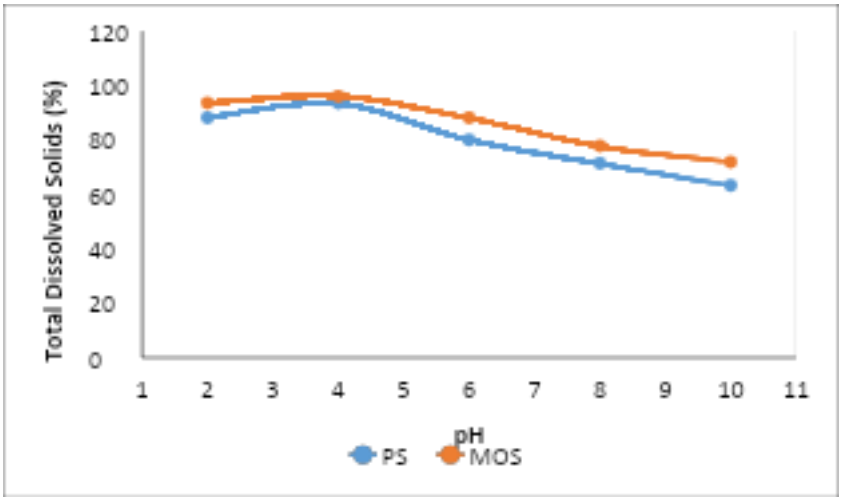

Table 4:
Optimum pH and pHpzc of PS and MOS values

Bio-coagulant	Optimum pH	pHpzc
PS	4.00	7.60
MOS	4.00	8.25

3.2.2 pH point of zero charge (pHpzc)

The pHpzc of PS and MOS was calculated using the pH drift method to be 7.60 and 8.25 correspondingly (Table 4 and Figure 2). These values suggest that both of the bio-coagulants were positively charged at the optimum pH due to protonation of the functional groups on the bio-coagulants surfaces. This agrees with the results of Ali et al. [31] who found that the adsorption of anions is favored when pH < pHpzc, whereas the adsorption of cations is preferred at pH > pHpzc. Thus, in this investigation with pH < pHpzc, the pHpzc value of MOS (8.25) shows that MOS has a stronger positive surface charge at a wider pH range, resulting in a greater adsorption contribution to TDS removal than PS.

Figure 2:
Point of zero charge (pHpzc) of (a) PS and (b) MOS (b) used for TDS adsorption

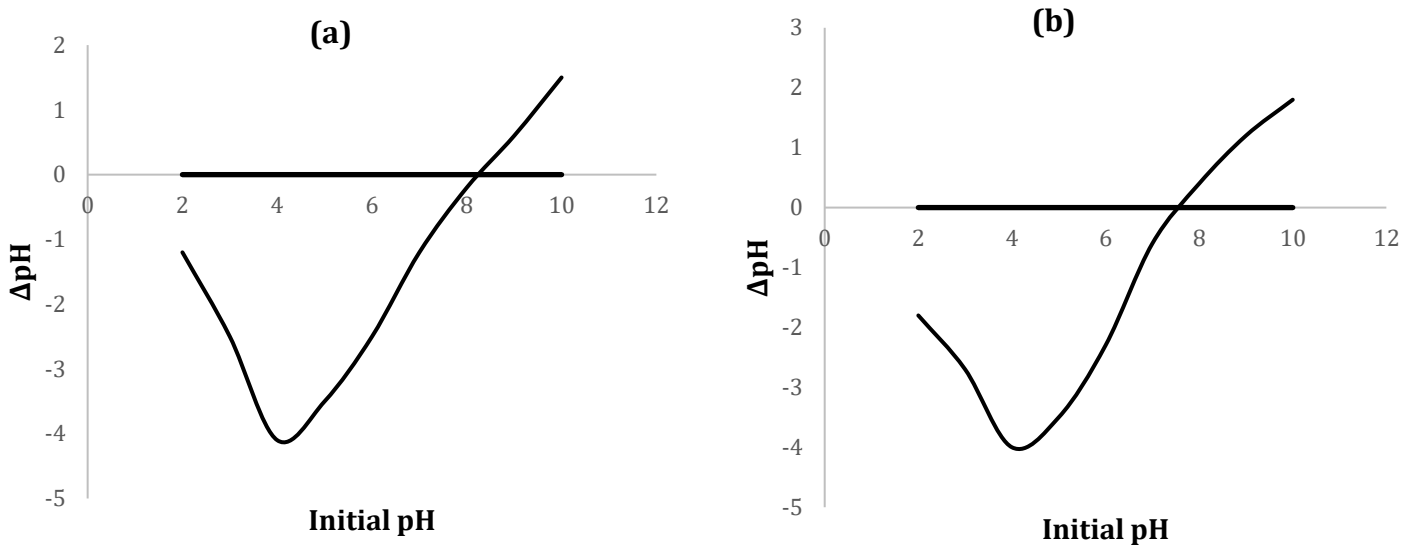

3.2.3 Effects of dosage on TDS removal

As presented in Figure 3, both PS and MOS achieved the highest TDS elimination at a dose of 4 g for the various coagulant dosages of 1–5 g and started decreasing thereafter. PS consistently performed slightly worse than MOS at all dosages. The first observed increase is due to the presence of active sites and charge-neutralizing species, which facilitate particle destabilization, bridging, and the development of denser flocs, thereby boosting removal efficiency, according to Al-Hanaktah et al. [32].

Figure 3:
Plot of TDS removal efficiency against dosage for PS and MOS bio-coagulants

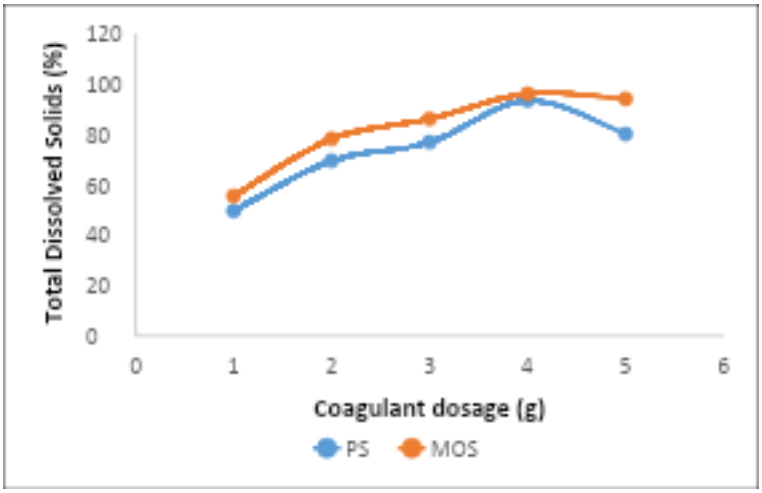

3.2.4 Effect of contact time on TDS removal

The removal of TDS in Figure 4 showed a sharp increase from 10 to 40 min and thereafter reached a near-equilibrium state for both PS and MOS. The rapid initial increase was due to the availability of abundant active sites and the strong concentration gradient between the wastewater and the surface of the bio-coagulant, similar to the reports of Pushpalatha et al. [33]. Similar to the previous results, MOS demonstrated slightly higher removal efficiencies than PS during the contact period which confirms the increased availability of the active functional groups for interaction with the pollutants [32, 33].

Figure 4:
Plot of TDS removal efficiency against contact time for PS and MOS bio-coagulants

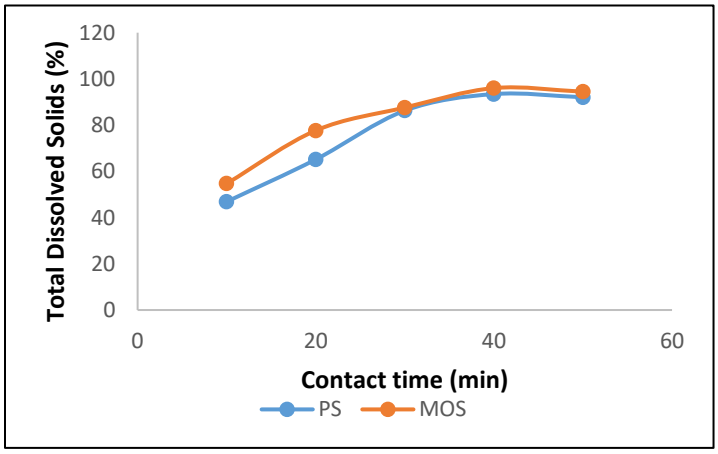

3.2.5 Validation of Optimum Operating Conditions

Table 5 shows the validation of results for optimum dosage, optimum pH and optimum contact time, and predicted and experimental TDS removal efficiencies for PS and MOS respectively, together with their percentage deviations. There is a good agreement between the experimental and predicted TDS removal efficiencies as the percentage deviations for each bio-coagulant is less than 1% [34]. This is a confirmation of the adequacy, reliability, and reproducibility of the optimization model as stated by Obinna et al. [34].

Table 5
Validation of optimum operating conditions

Wastewater + Coagulant	Optimum Dosage (g)	Optimum pH	Optimum Time, (min)	Predicted (Optimum) ηTDS, %	Experimental ηTDS,%	Percentage deviation, %
PWW + PS	4.00	4.00	40.00	93.53	92.87	0.71
PWW + MOS	4.00	4.00	40.00	97.24	96.49	0.78

3.3 Effect of Contact Time on Adsorption Capacity

Effect of contact time on the adsorption capacity (qt) for PS and MOS coagulants are shown in Figure 5. In both cases a quick uptake is observed in the first 20–30 min followed by a gradual attainment of the equilibrium between 40 and 50 min. The results suggest that the adsorption was a two-step process. The rapid initial rise of qt is consistent with the findings as reported in [5, 22] and was attributed to the occupation of the available active sites on the bio-coagulant surfaces. This can be related to the presence of key functional groups (–OH, –COOH and –NH) and surface charge effects that promote the attraction of dissolved ions [5, 30]. After 40 min, the adsorption rate decreased and qt approached equilibrium. This suggests that most of the readily available binding sites have been occupied and intra-particle diffusion is now the rate limiting phase. The difference in the maximum adsorption capacity measured for MOS (95.01 mg/g) and for PS (93.01 mg/g) is related to their protein contents and the density of cationic sites that increase the interactions with negatively charged species in the wastewater sample [22, 30]. This behavior shows the combined effect of surface adsorption and intra-particle diffusion mechanisms on the efficient TDS removal.

Figure 5:
Plot of adsorption capacity (q_t) against contact time

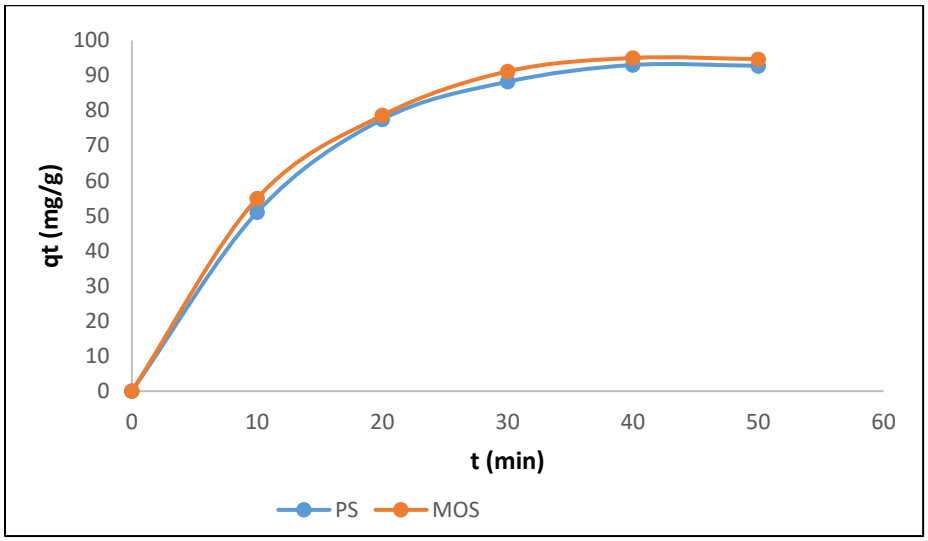

3.4 Adsorption Kinetics and Diffusion Analysis

The adsorption kinetics of TDS removal by PS and MOS were evaluated using pseudo-first-order, pseudo-second-order, Elovich, and Weber–Morris intra-particle diffusion models and the resulting parameters are summarized in Table 6. The combined kinetic and diffusion results suggest that TDS removal by both bio-coagulants occurred through a multi-step adsorption process involving surface interactions and mass-transfer effects, with the pseudo-second-order model providing the most suitable description of the adsorption behaviour.

3.4.1 Pseudo-first-order model

The pseudo-first-order model shown in Figure 6 provided relatively high-rate constants (k_1 = 0.5055 min^{-1} for PS and 0.6630 min^{-1} for MOS) but low correlation coefficients (R2 = 0.7160 for PS and R2 = 0.7968 for MOS) indicating that it did not sufficiently describe the adsorption process [5], [19].

Figure 6: Pseudo-first-order model plot for PS and MOS bio-coagulants

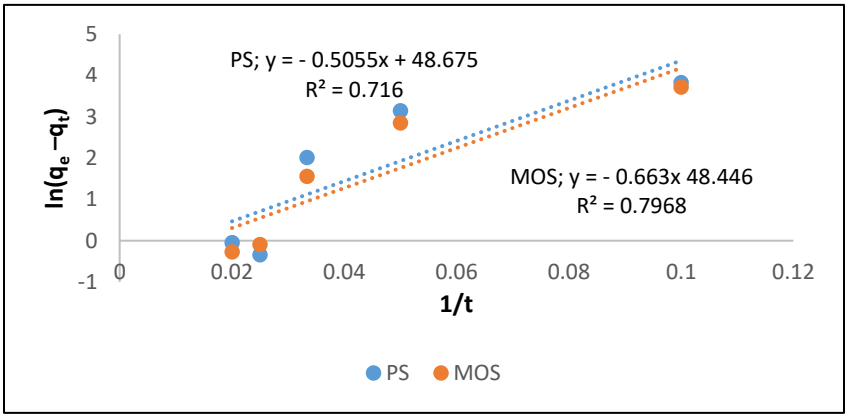

3.4.2 Pseudo-second-order model

The pseudo-second-order model (Figure 7) was found to be the best fit (R^2 = 0.9899 for PS and 0.9925 for MOS) with equilibrium adsorption capacities of 123.46 and 117.65 mg/g and rate constants of 0.000549 and 0.000847 g mg^{-1} min^{-1} for PS and MOS, respectively, indicating that surface adsorption was the dominant mechanism for TDS removal [19], [20], [35].

Figure 7:
Pseudo-second-order model for PS and MOS bio-coagulants

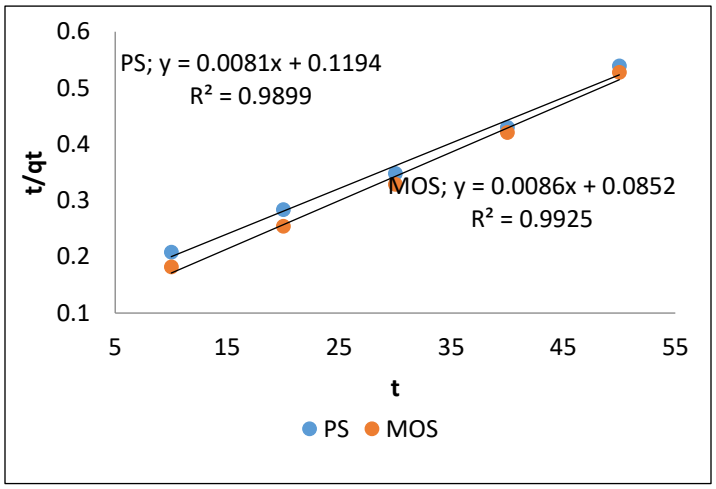

3.4.3 Elovich model

The Elovich model (Figure 8) parameters further revealed appreciable initial adsorption rates of α = 15.84 and 24.31 mg g^{-1} min^{-1} for PS and MOS, respectively with better fit (R^2) than the pseudo-first-order model and the Weber–Morris intra-particle diffusion model. This result confirmed the presence of energetically heterogeneous adsorption sites [19], [20].

Figure 8:
Elovich model plot for PS and MOS bio-coagulants

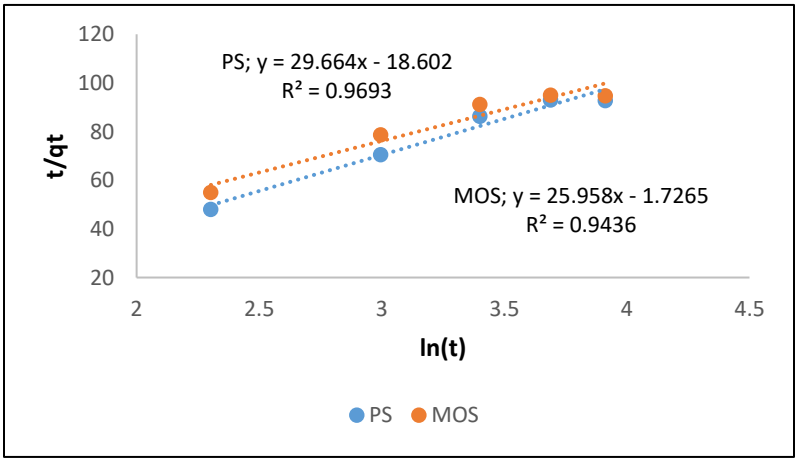

3.4.4 Weber–Morris intra-particle diffusion model

The constants of the Weber–Morris diffusion model (Figure 9) revealed a slightly higher intra-particle diffusion rate for PS (k_id = 11.961 mg g^{-1} $min^{-0.5}$) than for MOS (10.348 mg g^{-1} $min^{-0.5}$), while the higher intercept value for MOS (C = 28.039 mg/g) indicated a greater effect of the boundary-layer diffusion [19], [21].

Figure 9:
Weber–Morris intra-particle diffusion model plot for PS and MOS bio-coagulants

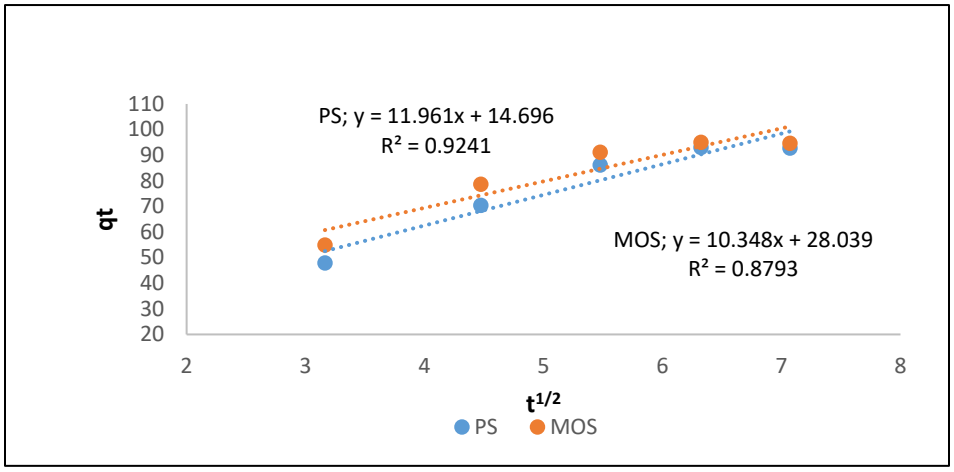

Table 6
Adsorption kinetic and intra-particle diffusion model Parameters

Model	Parameters	PS	MOS	R^2(PS)	R^2(MOS)
Pseudo-first-order	k_1 (min^{-1})	0.5055	0.6630	0.716	0.7968
Pseudo-second-order	qe (mg/g)	123.46	117.65	0.9899	0.9925
	k_2 (g mg^{-1} min^{-1})	0.000549	0.000847		
Elovich	α (mg g^{-1} min^{-1})	15.84	24.31	0.9693	0.9436
	β (g mg^{-1})	0.0337	0.0385	-	-
Intra-particle diffusion	kid (mg g^{-1} $min^{-0.5}$)	11.961	10.348	0.9241	0.8793
	C (mg/g)	14.696	28.039	-	-

3.5 Adsorption Isotherm Analysis

The adsorption equilibrium data for TDS removal by PS and MOS were fitted to Langmuir, Freundlich and Temkin isotherm models and the resultant model parameters are reported in Table 7. The better fit of the Langmuir model along with the positive values of the Freundlich and Temkin parameters shows that the TDS removal by PS and MOS mostly occurred via monolayer

adsorption with heterogeneous surface contacts and incremental variations in the energy of adsorption. [15], [23].

3.5.1 Langmuir model

The Langmuir model (Figure 10) produced higher correlation coefficients ($R^2 = 0.9935$ for PS and 0.9921 for MOS) compared to other isotherm models. From the derived model parameters in Table 7, the Langmuir maximum adsorption capacities of 55.56 mg/g for PS and 53.19 mg/g for MOS demonstrate the strong affinity of both bio-coagulants for dissolved solids [23], [24].

Figure 10:
Langmuir model plot for PS and MOS bio-coagulants

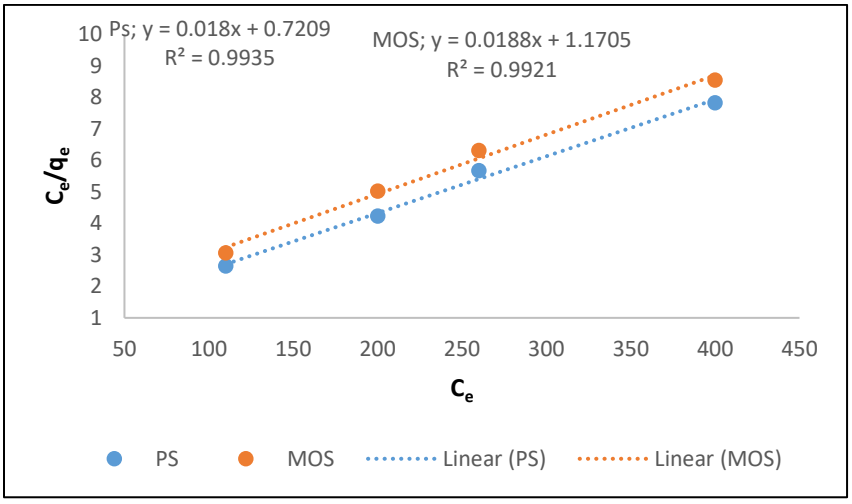

3.5.2 Freundlich model

The Freundlich model (Figure 11) with favourable parameters $R^2 = 0.9758$ for PS, $R^2 = 0.9588$ for MOS and the adsorption intensity parameter, $n>1$ for both bio-coagulants indicate favorable adsorption and suggest the presence of heterogeneous adsorption sites [15], [24].

Figure 11:
Freundlich model plot for PS and MOS bio-coagulants

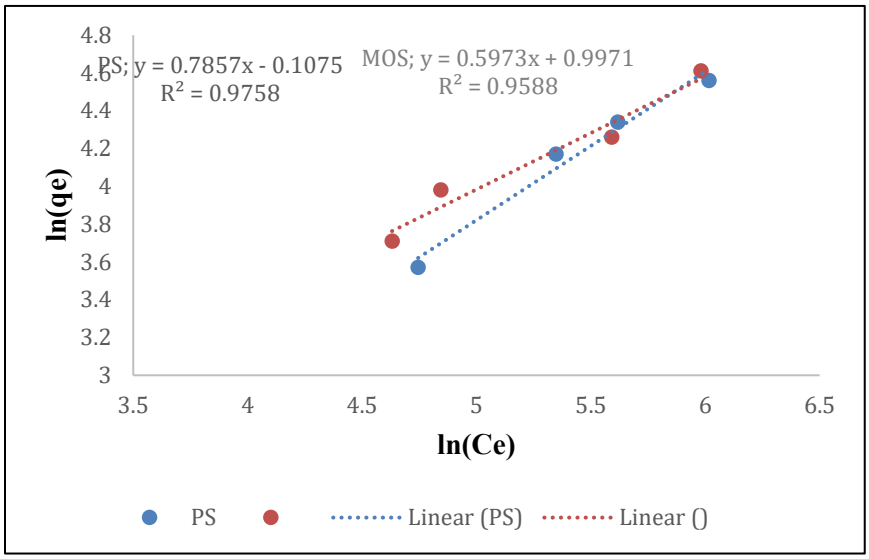

3.5.3 Temkin model

The Temkin model proposed that adsorption process is affected by adsorbent-adsorbate interactions and the heat of adsorption reduced gradually with increasing the surface covering [23], [24]. As shown in Figure 12, both PS and MOS exhibited good linear relationships (R^2 = 0.9775 and 0.9537, respectively), indicating that the Temkin model adequately describes the adsorption behaviour of the bio-coagulants.

Figure 12:
Temkin model plot for PS and MOS bio-coagulants

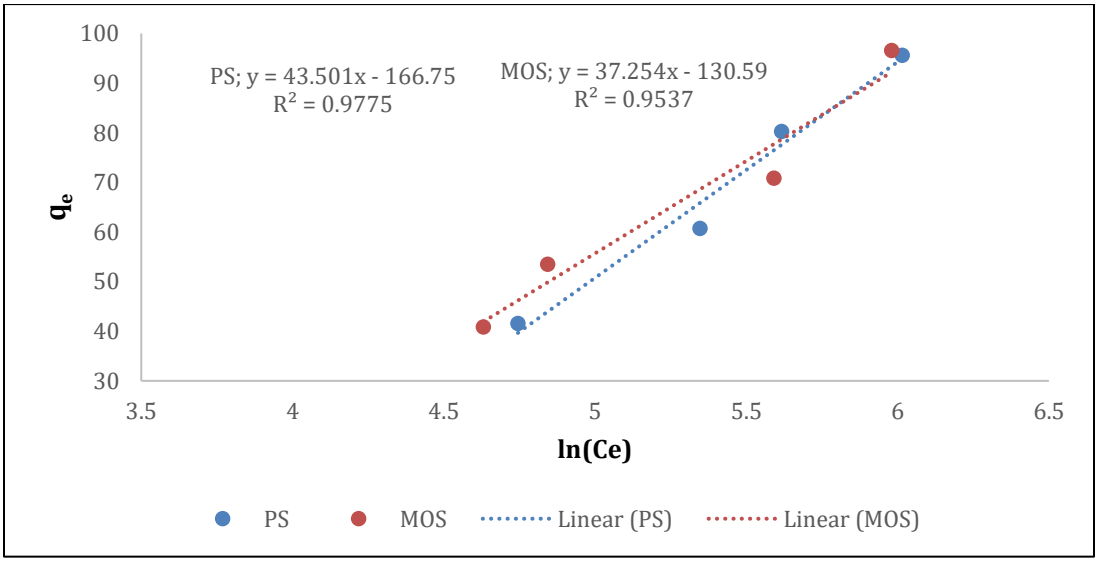

Table 7
Adsorption isotherm model parameters

Model	Parameters	PS	MOS	R^2(PS)	R^2(MOS)
Langmuir	q_{max} (mg/g)	55.56	53.19	0.9935	0.9921
	KL (L/mg)	0.0250	0.0161	-	-
Freundlich	Kf	0.898	2.710	0.9758	0.9588
	N	1.273	1.674	-	-
Temkin	B	43.501	37.254	0.9775	0.9537
	A (L/g)	0.0216	0.0300	-	-

3.6 Mechanistic Interpretation of TDS Removal by PS and MOS Bio-coagulants

The adsorption-assisted coagulation–flocculation mechanism of PS and MOS for TDS removal is shown in Figure 13. The treatment procedure starts with the addition of bio-coagulants into paint wastewater containing dissolved ions and colloidal species. The FTIR and proximate investigations indicated the presence of functional groups, protein and carbohydrate which are capable of interacting with dissolved contaminants and responsible for charge neutralization. The greater pHpzc values of both bio-coagulants relative to optimum treatment pH are consistent with protonation of surface functional groups and enhanced electrostatic attraction for negatively charged dissolved species. The protonated functional groups on PS and MOS favoured charge neutralization of dissolved species, leading to the development of bigger aggregates through coagulation–flocculation and particle-bridging mechanisms. However, coagulation-flocculation alone did not fully account for the total removal of dissolved particles. Residual dissolved species, after floc formation, were transported from the bulk solution to the bio-coagulant surface by boundary-layer and intra-particle diffusion processes, as described by the Weber–Morris model. This diffusion stage allowed contaminants to access the available active sites, thereby enabling further adsorption. Residual dissolved ions and molecules were retained on the bio-coagulant surface during the adsorption stage, as shown by the best fits of the pseudo-second-order kinetic and the Langmuir isotherm models. This reduces the concentration of particles in the aqueous phase and contributes to the overall reduction of TDS in the treated wastewater.

Figure 13:
Schematic illustration of the adsorption-assisted coagulation–flocculation mechanism responsible for TDS removal by PS and MOS.

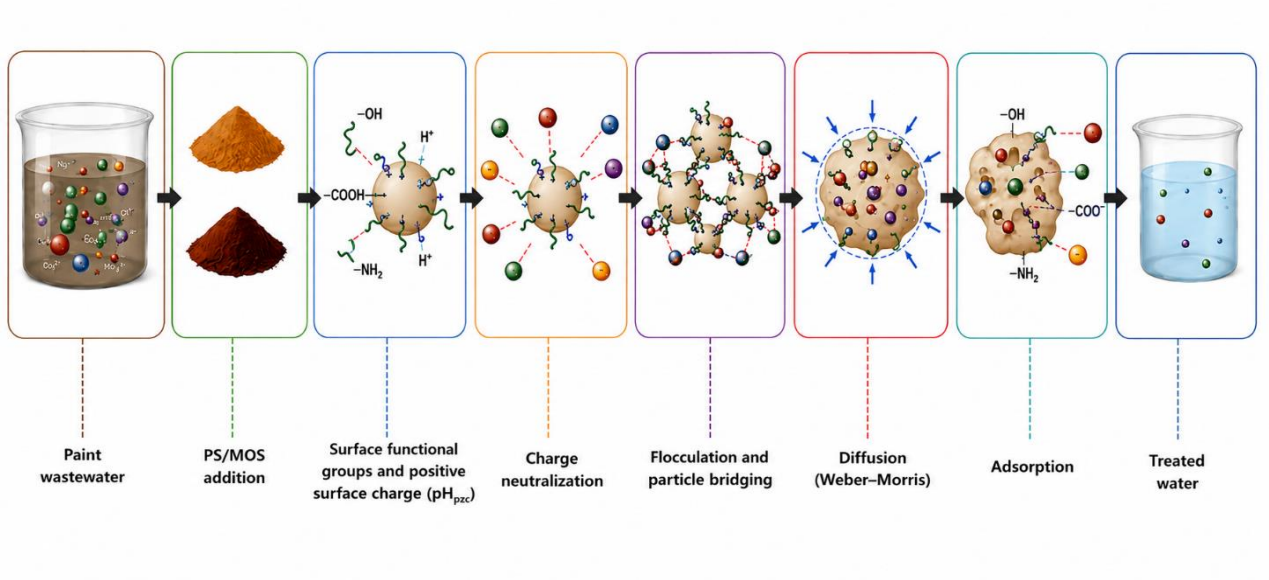

3.7 The Superior Performance of MOS Over PS

A critical observation of Table 8 clearly shows why MOS outperformed PS even though PS exhibited faster diffusion, slightly higher theoretical adsorption capacity and stronger adsorption–model correlations. MOS achieved higher TDS removal because its protein-rich composition provided more cationic active sites. MOS's higher pHpzc resulted in a stronger positive surface charge at optimum pH, which enhanced charge neutralization, destabilization of dissolved species and floc formation through coagulation–flocculation and particle bridging before the adsorption became significant. So, we affirm that adsorption favoured PS slightly, whereas coagulation–flocculation favoured MOS more strongly. Since the treatment process was primarily coagulation–flocculation based, MOS achieved the better overall performance. On the contrary, had the treatment process been based solely on adsorption, PS would likely have demonstrated superior overall TDS removal efficiency.

Table 8
Comparative summary of key performance and mechanistic parameters of PS and MOS

Parameter	PS	MOS	Better Performer
Protein content (%)	18.96	37.16	MOS
Carbohydrate content (%)	53.08	44.63	PS
pHpzc	7.60	8.25	MOS
Optimum pH	4	4	Similar

Optimum dosage (g)	4	4	Similar
Optimum contact time (min)	40	40	Similar
TDS removal at optimum conditions (%)	93.0	96.0	MOS
Final TDS concentration (mg/L)	165.54	100.13	MOS
Experimental equilibrium adsorption capacity, qt,max (mg/g)	93.01	95.01	MOS
Langmuir adsorption capacity, qmax (mg/g)	55.56	53.19	PS
Langmuir R^2	0.9935	0.9921	PS
Freundlich R^2	0.9758	0.9588	PS
Temkin R^2	0.9775	0.9537	PS
Pseudo-second-order R^2	0.9899	0.9925	MOS
Pseudo-second-order qe (mg/g)	123.46	117.65	PS
Pseudo-second-order k_2 (g mg^{-1} min^{-1})	0.000549	0.000847	MOS
Pseudo-first-order R^2	0.7160	0.7968	MOS
Pseudo-first-order k_1 (min^{-1})	0.5055	0.6630	MOS
Elovich R^2	0.9693	0.9436	PS
Weber–Morris R^2	0.9241	0.8793	PS
Intra-particle diffusion constant, kid (mg g^{-1} $min^{0.5}$)	11.96	10.35	PS
Boundary-layer constant, C (mg/g)	14.70	28.04	MOS
Dominant diffusion characteristic	Faster internal diffusion	Stronger film diffusion effect	Different mechanisms
Overall treatment performance	High	Higher	MOS

Experimental equilibrium adsorption capacity (qt,max) was obtained from the contact-time study, whereas Langmuir qmax represents the theoretical monolayer adsorption capacity estimated from equilibrium isotherm modelling.

3.8 Comparison with Literature

The results of the present investigation are comparable with other plant-based coagulants used in industrial wastewater treatment as depicted in Table 9 [28, 36-40]. In addition to their high removal performance, PS and MOS offer advantages such as low cost, biodegradability, and local availability. These characteristics support their potential application as sustainable alternatives for industrial wastewater treatment. The study provides deeper adsorption-assisted coagulation–flocculation mechanistic understanding for TDS removal. However, the present study was limited

to batch-scale research and did not include advanced surface characterization, thermodynamic evaluation and bio-coagulant regeneration tests.

Table 9
Compares TDS removal efficiency of PS and MOS to other bio-coagulants reported in literature

Bio-coagulant Type	Wastewater Type	TDS Removal (%)	Reference
Pear seed (PS)	Paint wastewater	93	This study
Moringa oleifera seed (MOS)	Paint wastewater	96	This study
Aloe vera	Brewery wastewater	95.40	[28]
Cactus opuntia	Brewery wastewater	95	[28]
Okra seeds	Brewery wastewater	95.25	[28]
Blend: Aloe vera + Cactus opuntia + Okra seeds	Brewery wastewater	95.12	[28]
Moringa oleifera seed powder	Abandoned mining pond water	23.08	[36]
Watermelon seed coagulant + Alum (1:3 ratio)	Gibe River wastewater	98.26	[37]
Carica papaya leaf coagulant	Mechanic village seep water	84.34	[38]
Moringa oleifera seed	Mechanic village seep water	93.72	[38]
Seamum indicum seed extract	Aquaculture wastewater	82	[39]
Okra seeds	Tannery wastewater	69	[40]

4. Conclusion

In this study, both bio-coagulants achieved high treatment efficiencies, with MOS exhibiting superior overall performance than PS. The integration of FTIR, pHpzc, kinetic, diffusion, and isotherm analyses enabled the development of a mechanistic pathway in which charge neutralization and flocculation constituted the primary removal processes, while diffusion and adsorption contributed to the further removal of dissolved solids that remained after coagulation–flocculation. The findings highlight the potential of PS and MOS as low-cost, biodegradable, and

environmentally sustainable alternatives to conventional chemical coagulants for industrial wastewater treatment. Future studies should investigate the regeneration and reuse of the bio-coagulants, evaluate their performance under continuous-flow and pilot-scale conditions, and assess sludge characteristics and treatment economics. Additional surface characterization techniques such as SEM, BET, thermodynamic and zeta potential analyses may further improve understanding of the adsorption-assisted coagulation–flocculation mechanism and support large-scale implementation.

List of Abbreviations

BET – Brunauer–Emmett–Teller method
BOD_5 – Biological Oxygen Demand (5-day)
COD – Chemical Oxygen Demand
EDTA – Ethylenediaminetetraacetic Acid
FTIR – Transform Infrared Spectroscopy
MOS – *Moringa oleifera* Seed
NTU – Nephelometric Turbidity Unit
PFO – Pseudo-First-Order
PS – Avocado Pear Seed
PSO – Pseudo-Second-Order
PWW – Paint Wastewater
pHpzc – pH Point of Zero Charge
SEM – Scanning Electron Microscopy
TDS – Total Dissolved Solid
TS – Total Solids
TSS – Total Suspended Solids

Nomenclature (Symbols)

k_1 – Pseudo-first-order rate constant (min^{-1})
k_2 – Pseudo-second-order rate constant (g mg^{-1} min^{-1})
K_F – Freundlich adsorption capacity constant
n – Freundlich adsorption intensity parameter
K_L – Langmuir adsorption constant (L mg^{-1})
C_0 – Initial TDS concentration (mg L^{-1})
C_t – Final TDS concentration (mg L^{-1})
C_e – Equilibrium TDS concentration (mg L^{-1})
q_t – Adsorption capacity at time (mg g^{-1})
q_e – Equilibrium adsorption capacity
q_m – Maximum adsorption capacity (mg g^{-1})
α – Elovich initial adsorption rate constant (mg g^{-1} min^{-1})
β – Elovich desorption constant (g mg^{-1})
A_T – Temkin equilibrium binding constant (L g^{-1})
B – Temkin constant related to heat of adsorption (J mol^{-1})
C – Intraparticle diffusion intercept (boundary layer thickness constant) (mg g^{-1})

R^2 – Coefficient of determination

Author Contributions

Conceptualization, C.O.A and O.S.N; methodology, C.O.A and O.S.N; software, C.O.A; validation, C.O.A, and O.C.N; formal analysis, C.O.A and O.S.N; investigation, C.O.A; resources, O.S.N and O.C.N; data curation, C.O.A; writing – original draft preparation, C.O.A; writing – review and editing, C.O.A; visualization, C.O.A; supervision, O.S.N and O.C.N; project administration, O.S.N. All authors have read and agreed to the published version of the manuscript.

Availability of Data and Material

The data presented in this study are available on request from the corresponding author.

Funding

The authors received no financial support for the research, authorship or its publication.

Conflicts of Interest

The authors declare that there is no conflict of interests regarding the publication of this manuscript.

Acknowledgment

The authors acknowledge the Department of Chemical Engineering, Enugu State University of Science and Technology (ESUT), Enugu, Nigeria, for providing laboratory support for this study. The authors also acknowledge Nigerian Breweries Plc., Enugu State, Nigeria, for granting access to the brewery wastewater samples used in this research.

AI Declaration

The authors confirm that no AI tools were used to generate any part of the manuscript text, including the research design, data collection, data analysis, interpretation of the findings, and manuscript preparation and revision.

References

[1] Viktoryová, N., Szarka, A., & Hrouzková, S. (2022). Recent developments and emerging trends in paint industry wastewater treatment methods. *Applied sciences*, *12*(20), 10678.

[2] Yadav, D., & Dutta, J. (2024). Advancing environmental sustainability: recent trends and developments in treatment methods for paint industry wastewater. *Journal of Water Process Engineering*, *61*, 105290.

[3] Nair, S., Manu, B., & Azhoni, A. (2021). Sustainable treatment of paint industry wastewater: Current techniques and challenges. *Journal of Environmental Management*, *296*, 113105.
[4] Al-Jadabi, N., Laaouan, M., El Hajjaji, S., Mabrouki, J., Benbouzid, M., & Dhiba, D. (2023). The dual performance of Moringa oleifera seeds as eco-friendly natural coagulant and as an antimicrobial for wastewater treatment: a review. *Sustainability*, *15*(5), 4280.
[5] Varsani, V. G., Vyas, S. J., Parmar, V., Dudhagara, D., Gamit, S., Ali, D., ... & Patel, A. (2024). Efficient and eco-friendly treatment of wastewater through sustainable purification using agricultural waste and coagulation kinetic modelling. *Frontiers in Environmental Science*, *11*, 1280125.
[6] Miyah, Y., El Messaoudi, N., Benjelloun, M., Acikbas, Y., Şenol, Z. M., Ciğeroğlu, Z., & Lopez-Maldonado, E. A. (2024). Advanced applications of hydroxyapatite nanocomposite materials for heavy metals and organic pollutants removal by adsorption and photocatalytic degradation: A review. *Chemosphere*, *358*, 142236.
[7] Jabar, J. M., Odusote, Y. A., Alabi, K. A., & Ahmed, I. B. (2020). Kinetics and mechanisms of congo-red dye removal from aqueous solution using activated Moringa oleifera seed coat as adsorbent. *Applied Water Science*, *10*(6), 1-11.
[8] Zhang, Y., Li, M., Zhang, G., Liu, W., Xu, J., Tian, Y., ... & Xie, X. (2023). Efficient treatment of the starch wastewater by enhanced flocculation–coagulation of environmentally benign materials. *Separation and Purification Technology*, *307*, 122788.
[9] Koul, B., Bhat, N., Abubakar, M., Mishra, M., Arukha, A. P., & Yadav, D. (2022). Application of natural coagulants in water treatment: a sustainable alternative to chemicals. *Water*, *14*(22), 3751.
[10] Badawi, A. K., Salama, R. S., & Mostafa, M. M. M. (2023). Natural-based coagulants/flocculants as sustainable market-valued products for industrial wastewater treatment: a review of recent developments. *RSC advances*, *13*(28), 19335-19355.
[11] Obiora-Okafo, I. A., Onukwuli, O. D., & Eli-Chukwu, N. C. (2020). Evaluation of bio-coagulants for colour removal from dye synthetic wastewater: characterization, adsorption kinetics, and modelling approach. *Water SA*, *46*(2), 300-312.
[12] Zhou, Z., Yu, T., Dong, H., Huang, L., Chu, R. K., Tolic, N., ... & Zeng, Q. (2019). Chemical oxygen demand (COD) removal from bio-treated coking wastewater by hydroxyl radicals produced from a reduced clay mineral. *Applied Clay Science*, *180*, 105199.
[13] Arris, S., Ayat, A., Bencheikh-Lehocine, M., & Meniai, A. H. (2021). Removal of turbidity and chemical oxygen demand using an eco-friendly coagulant/flocculent (optimization and modeling through the response surface methodology). *Desalination and Water Treatment*, *211*, 338-348.
[14] Mogbo, O. N., Iorwua, M. B., Duweni, E. C., & Tiza, M. T. (2020). A study on the efficacy of bio-coagulants for turbid and waste water treatment. *J. Crit. Rev*, *7*, 1307-1315.
[15] Okolo, B. I., Oke, E. O., Adeyi, O., Akatobi, K. N., & Dzarma, G. W. (2021). Adsorption isotherm, kinetic and thermodynamic studies for removal of total dissolved solid from paint wastewater using acid modified mucuna shell. *Lautech Journal of Engineering and Technology*, *15*(1), 53-74.
[16] Revellame, E. D., Fortela, D. L., Sharp, W., Hernandez, R., & Zappi, M. E. (2020). Adsorption kinetic modeling using pseudo-first order and pseudo-second order rate laws: A review. *Cleaner Engineering and Technology*, *1*, 100032.

[17] Mohamed Nasser, S., Abbas, M., & Trari, M. (2024). Understanding the rate-limiting step adsorption kinetics onto biomaterials for mechanism adsorption control. *Progress in Reaction Kinetics and Mechanism*, *49*, 14686783241226858.
[18] Moussout, H., Ahlafi, H., Aazza, M., & Maghat, H. (2018). Critical of linear and nonlinear equations of pseudo-first order and pseudo-second order kinetic models. *Karbala International Journal of Modern Science*, *4*(2), 244-254.
[19] Bujdák, J. (2020). Adsorption kinetics models in clay systems. The critical analysis of pseudo-second order mechanism. *Applied clay science*, *191*, 105630.
[20] Tseng, R. L., Tran, H. N., & Juang, R. S. (2022). Revisiting temperature effect on the kinetics of liquid–phase adsorption by the Elovich equation: A simple tool for checking data reliability. *Journal of the Taiwan Institute of Chemical Engineers*, *136*, 104403.
[21] Dharmarathna, S. P., & Priyantha, N. (2024). Investigation of boundary layer effect of intra-particle diffusion on methylene blue adsorption on activated carbon. *Energy Nexus*, *14*, 100294.
[22] Zehouani, I., Mandi, L., El Barkaoui, S., Sbahi, S., & Ouazzani, N. (2026). Adsorption capacity assessment of biochar from two agricultural wastes for urban and agri-food industrial wastewater treatment. *International Journal of Environmental Science and Technology*, *23*(2), 129.
[23] Shimizu, S., & Matubayasi, N. (2023). Understanding sorption mechanisms directly from isotherms. *Langmuir*, *39*(17), 6113-6125. https://doi.org/10.1021/acs.langmuir.3c00256
[24] Amrutha, Jeppu, G., Girish, C. R., Prabhu, B., & Mayer, K. (2023). Multi-component adsorption isotherms: review and modeling studies. *Environmental processes*, *10*(2), 38. https://doi.org/10.1007/s40710-023-00631-0
[25] Onyekachi Stephen Nnamani, Benson Chinweuba Udeh, Cyprian Obinna Azinta. (2026). Data-Driven Optimization of Plant-Derived Bio-Coagulants for TDS Removal from Paint Wastewater: Comparative RSM and ANN Modeling. *Sustainable Processes Connect*, 2 (Article ID: 0028). https://doi.org/Registering DOI
[26] Obiora-Okafo, I. A., & Onukwuli, O. D. (2017). Optimization of coagulation-flocculation process for colour removal from azo dye using natural polymers: Response surface methodological approach. *Nigerian Journal of Technology*, *36*(2), 482-495.
[27] Stadtlander, T., & Becker, K. (2017). Proximate composition, amino and fatty acid profiles and element compositions of four different Moringa species. *Journal of Agricultural Science*, *9*(7), 46-57.
[28] Murisa, V., Ncube, S., Moyo, L. B., Danha, G., & Mamvura, T. A. (2024). Treatment of effluent from a malting processing plant using bio-coagulants. *Discover Civil Engineering*, *1*(1), 29. https://doi.org/10.1007/s44290-024-00030-w
[29] Arasaretnam, S., & Keerthanan, S. (2018). Plant seeds as biosorbents for the purification of water. *Journal of Modern Chemistry & Chemical Technology*, *9*(2), 30-39.
[30] Crini, G. (2005). Recent developments in polysaccharide-based materials used as adsorbents in wastewater treatment. *Progress in polymer science*, *30*(1), 38-70.
[31] Ali, S. K., Abdou, M. M., Emara, M. M., Farag, R. S., & Mubarak, M. F. (2025). Eco-friendly solutions: a comprehensive review of natural coagulants for sustainable water treatment. *Environmental Geochemistry and Health*, *47*(12), 535.
[32] Al-Hanaktah, A., Al-Rafayia, R. A., Ala'Haitham, A. G., Al-Rawajfeh, A. E., Mainali, B., & Shahid, M. K. (2025). A comparative analysis of defatted pumpkin seed extract and

conventional coagulants for sustainable turbidity reduction in water and wastewater treatment. *Cleaner Water*, 100114.
[33] Pushpalatha, N., Sreeja, V., Karthik, R., & Saravanan, G. (2022). Total dissolved solids and their removal techniques. *International Journal*, *2*(2), 13-20.
[34] Obinna, A. C., Mbah, G. O., & Onoh, M. I. (2021). Optimization and process modeling of viscosity of oil based drilling muds. *Journal of Human, Earth, and Future*, *2*(4), 412-423.
[35] Wu, F. C., Tseng, R. L., Huang, S. C., & Juang, R. S. (2009). Characteristics of pseudo-second-order kinetic model for liquid-phase adsorption: A mini-review. *Chemical Engineering Journal*, *151*(1-3), 1-9.
[36] Sunday, D. B., Hassan, I. & Aliyu, S. (2025). Performance Evaluation and Optimization of Moringa Oleifera Seed Powder as Bio-Coagulant for Water Purification in Jos Mining Pond. Engineering Research Journal. 5(4), 81-99. https://doi.org/10.5281/zenodo.17982980
[37] Endale, Y., Samuel, Z. A., Kebede, S., & Bayu, A. B. (2024). Blended natural and synthetic coagulants for the COD and BOD removal from surface water; optimization by response surface methodology: The case of Gibe river. *Heliyon*, *10*(18).
[38] Ifegbo, A. N., Onukwuli, O. D., & Obiora-Okafo, I. A. (2022). Comparative study of adsorption characteristics of coag-flocculation performances of bio-coagulants in mechanic village seeped water medium. *Journal of Engineering and Applied Sciences*, *21*(1), 922-941.
[39] Lee, C. S., Chong, M. F., Robinson, J., & Binner, E. (2014). A review on development and application of plant-based bioflocculants and grafted bioflocculants. *Industrial & Engineering Chemistry Research*, *53*(48), 18357-18369.
[40] Agarwal, M., Rajani, S., Mishra, A., & Rai, J. S. P. (2003). Utilization of okra gum for treatment of tannery effluent. *International Journal of Polymeric Materials*, *52*(11-12), 1049-1057.